Doublet structure in the absorption coefficient for tunneling-split intersubband transitions in double quantum wells

Godfrey Gumbs*
Department of Physics and Astronomy, Hunter College of the City University of New York, 695 Park Avenue, New York, New York 10021

Danhong Huang
Department of Electrical and Computer Engineering, Wayne State University, Detroit, Michigan 48202

D. N. Talwar
Department of Physics, 56 Weyandt Hall, Indiana University of Pennsylvania, Indiana, Pennsylvania 15705-1087

(Received 13 April 1995; revised manuscript received 14 February 1996)

Calculations of the absorption coefficient for tunneling-split intersubband transitions in double quantum wells are presented and the line shape is analyzed as a function of the temperature and dopant concentration. The peaks in the absorption coefficient correspond to tunneling-split intersubband transitions resulting in the resonant absorption of light. The lower-energy absorption peak is induced by electron tunneling. This doublet structure accounts for the transitions between the tunneling-split originally degenerate ground-state subbands in the isolated quantum wells and corresponds to the transition from the Fermi edge of the lower tunneling-split subband and the transition to the Fermi edge of the upper tunneling-split subband. These two transitions are unresolved at low temperatures but become resolved at high temperatures. When the dopant charge density is increased, the absorption peak strength increases. It also brings out another unresolved absorption peak due to the transition between tunneling-split excited states. [S0163-1829(96)01320-3]

There is now a broad interest in double quantum wells (DQW's) in the presence and absence of an external magnetic field. We are interested here in the frequency-dependent absorption coefficient of DQW's. The quasiparticle energy is calculated in the self-consistent Hartree approximation, including electron tunneling. The effect of a subband-dependent electron effective mass for the quantized energy levels within the wells is also considered. When the electron gas with a positive jellium background is perturbed by an external electric field, the induced density fluctuation of the electrons will oscillate with a normal mode frequency. It introduces into a collective dipole moment in the system. We present a theory for the absorption coefficient in the DQW's structure when an induced collective dipole moment in the system is included by a self-consistent equation. The coupling of the total dipole to the external electric field gives rise to energy absorption, which is represented by the absorption coefficient we derive in this paper. The polarization of the electric field is assumed in the z direction, parallel to the growth axis so that the tunneling-split intersubband transitions of the DQW's can be excited. Zaluzny[1,2] did a considerable amount of work on the spectral line shape of intersubband transitions in single quantum wells. His results show that when the effective masses of the quantized levels are energy dependent, the peak positions and line shape are affected. In a recent paper, Gumbs, Huang, and Loehr[3] calculated the temperature dependence of the peak positions of the absorption coefficient of a single quantum well. Gumbs and Aizin[4] also calculated the tunneling density of states and plasmon excitations of a DQW's in the absence of a magnetic field and the magnetoplasmon and Bernstein-like modes in a perpendicular magnetic field.[5] We consider tunneling-split intersubband transitions and describe the eigenfunctions by $\Psi_{n,\vec{k}_{||}}(\vec{r})=\exp(i\vec{k}_{||}\cdot\vec{r}_{||})\zeta_n(z)/\sqrt{A}$ where n is the subband index, $\vec{r}=(\vec{r}_{||},z)$ is a position vector, $\vec{k}_{||}$ and $\vec{r}_{||}$ are two-dimensional (2D) vectors, A is the sample cross-sectional area. The confinement of an electron in the z direction within the double quantum wells leads to discrete energy subbands that are self-consistently determined by the Schrödinger and Poisson equations for the Hartree potential.[6–9]

We use linear response theory to obtain the absorption coefficient for the tunneling-split intersubband transitions in a double-quantum-well structure. A straightforward calculation shows that the absorption coefficient is given by

$$\beta_{\rm abs}(\omega)=[\omega/n(\omega)\epsilon_0 c][1+\rho_{\rm ph}(\omega)]{\rm Im}\alpha_L(\omega), \quad (1)$$

where Im indicates that the imaginary part must be taken, $\rho_{\rm ph}(\omega)=[\exp(\hbar\omega/k_BT)-1]^{-1}$ is the photon distribution factor, and $\alpha_L(\omega)$ is the Lorentz ratio (defined as the ratio of the Fourier coefficient of the absorbed energy at frequency ω of a probing field to the square of its amplitude) given by

$$\alpha_L(\omega)=\frac{-e}{|\vec{E}_{\rm ext}|}\frac{1}{AL_z}\sum_{q_{||}}\int d\vec{r}\,\delta n_{\rm ind}(\vec{r},\omega)\vec{r}\frac{\vec{E}_{\rm ext}}{|\vec{E}_{\rm ext}|}e^{-i\vec{q}_{||}\cdot\vec{r}_{||}}, \quad (2)$$

where $E_{\rm ext}$ is the amplitude of the external electric field. The length of the region containing DQW's is denoted by L_z and A is the sample cross-sectional area. The frequency-dependent refractive index $n(\omega)$ of the medium is defined by

$$n(\omega)=\frac{1}{\sqrt{2}}\left[\epsilon_b+\frac{{\rm Re}\alpha_L(\omega)}{\varepsilon_0}+\sqrt{\left(\epsilon_b+\frac{{\rm Re}\alpha_L(\omega)}{\varepsilon_0}\right)^2+\left(\frac{{\rm Im}\alpha_L(\omega)}{\varepsilon_0}\right)^2}\right]^{1/2}. \quad (3)$$

Here, ϵ_b is the averaged optical dielectric constant of the system, and Re denotes taking the real part.

The induced electron density has a planar Fourier transform that is given by

$$\delta n_{\rm ind}(\vec{q}'_{||},z;\omega)=\frac{2}{A}\sum_{n,\vec{k}_{||}}\sum_{n',\vec{k}'_{||}}F^{*}_{\vec{k}_{||},\vec{k}'_{||}}(\vec{q}'_{||})\Pi^{(0)}_{n,\vec{k}_{||},n',\vec{k}'_{||}}(\omega)$$
$$\times\sum_{\vec{q}_{||}}\{e\vec{E}^{\rm ext}\cdot\vec{r}_{n,\vec{k}_{||};n',\vec{k}'_{||}}(\vec{q}_{||})$$
$$+v_{\rm c}(q_{||})F_{\vec{k}_{||},\vec{k}'_{||}}(\vec{q}_{||})K_{nn'}(\vec{q}_{||},\omega)\}$$
$$\times\zeta_{n'}(z)\zeta_{n}(z), \tag{4}$$

where $v_{\rm c}(q_{||})$ is the 2D Fourier transform of the bare Coulomb potential,

$$\Pi^{(0)}_{n,\vec{k}_{||},n',\vec{k}'_{||}}(\omega)\equiv\frac{f_0(E_{n,\vec{k}_{||}})-f_0(E_{n',\vec{k}'_{||}})}{\hbar\omega-(E_{n',\vec{k}'_{||}}-E_{n,\vec{k}_{||}})+i\gamma}. \tag{5}$$

Here, $\gamma\rightarrow 0^{+}$ is a broadening parameter due to scattering, $f_0(E)$ is the Fermi function, and $E_{n,\vec{k}_{||}}=E_n+\hbar^2k_{||}^2/2m_n^*$ are the energy eigenvalues. Also, $F_{\vec{k}_{||},\vec{k}'_{||}}(\vec{q}_{||})\equiv\langle\vec{k}_{||}|e^{-i\vec{q}_{||}\cdot\vec{r}_{||}}|\vec{k}'_{||}\rangle$,

$$\vec{r}_{n,\vec{k}_{||};n',\vec{k}'_{||}}(\vec{q}_{||})\equiv\langle n,\vec{k}_{||}|\vec{r}e^{-i\vec{q}_{||}\cdot\vec{r}_{||}}|n',\vec{k}'_{||}\rangle, \tag{6}$$

$$K_{nn'}(\vec{q}_{||},\omega)\equiv\int_{-\infty}^{\infty}dz\int_{-\infty}^{\infty}dz'e^{-q_{||}|z-z'|}\zeta_n(z)\zeta_{n'}(z)$$
$$\times\delta n_{\rm ind}(\vec{q}_{||},z';\omega). \tag{7}$$

Equations (4) and (7) combine to give the self-consistent field equations for $K_{mm'}(\vec{q}'_{||},\omega)$ as

$$\sum_{n,n'}\left[\delta_{nm}\delta_{n'm'}-\frac{2}{A}\sum_{\vec{k}_{||}}\Pi^{(0)}_{n,\vec{k}_{||},n',\vec{k}_{||}+\vec{q}_{||}}\right.$$
$$\left.\times(\omega)U_{mm';nn'}(\vec{q}_{||},\vec{k}_{||})\right]\frac{K_{nn'}(\vec{q}_{||},\omega)}{|e\vec{E}^{\rm ext}|}$$
$$=\frac{2}{A}\sum_{n,n',\vec{k}_{||}}\Pi^{(0)}_{n,\vec{k}_{||},n',\vec{k}_{||}+\vec{q}_{||}}(\omega)I_{mm';nn'}(\vec{q}_{||})Z_{nn'}, \tag{8}$$

where

$$U_{mm';nn'}(\vec{q}_{||},\vec{k}_{||})=v_{\rm c}(q_{||})I_{mm';nn'}(q_{||}), \tag{9}$$

$$I_{mm';nn'}(q'_{||})\equiv\int_{-\infty}^{\infty}dz\int_{-\infty}^{\infty}dz'\zeta_m(z')\zeta_{m'}(z')$$
$$\times e^{-q'_{||}|z'-z|}\zeta_n(z)\zeta_{n'}(z), \tag{10}$$

$$Z_{nn'}\equiv\int_{-\infty}^{\infty}dz\zeta_n(z)z\zeta_{n'}(z). \tag{11}$$

After Eq. (8) is solved for the matrix elements $K_{n,n'}/|e\vec{E}^{\rm ext}|$, the results must be substituted into Eq. (4) to obtain the induced electron density. This result for $\delta n_{\rm ind}$ is then substituted into Eq. (2) for the Lorentz ratio. Calculation shows that

$$\alpha_L(\omega)=-\frac{2e^2}{AL_z}\sum_{n,n'}\sum_{\vec{k}_{||},\vec{q}_{||}}Z^{*}_{nn'}\Pi^{(0)}_{n,\vec{k}_{||},n',\vec{k}_{||}+\vec{q}_{||}}(\omega)$$
$$\times\{Z_{nn'}+v_{\rm c}(q_{||})K_{nn'}(\vec{q}_{||},\omega)/|e\vec{E}^{\rm ext}|\}. \tag{12}$$

Since the dipole matrix element $Z_{nn'}$ in Eq. (11) is finite only when $\zeta_n(z)$ and $\zeta_{n'}(z)$ have different spatial symmetry, the only allowed contributions to the Lorentz ratio in Eq. (12) and subsequently the absorption coefficient in Eq. (1) are between the symmetric and antisymmetric states. For single-particle excitations, the absorption coefficient in the long-wavelength limit has been calculated as

$$\alpha_L(\omega)=-(2e^2/L_z)\sum_{n,n'}|Z_{nn'}|^2\chi_{nn'}(\omega), \tag{13a}$$

$$\chi_{nn'}(\omega)\equiv(1/A)\sum_{\vec{k}_{||}}\Pi^{(0)}_{n,\vec{k}_{||},n',\vec{k}_{||}}(\omega). \tag{13b}$$

In particular, at $T=0$ K, we obtain

$$\mathrm{Re}\chi_{nn'}(\omega)=\frac{1}{4\pi b}\ln\left[\frac{\hbar^4(\omega^2-\omega_1^2)^2+4\gamma^2\hbar^2\omega^2}{\hbar^4(\omega^2-\omega_2^2)^2+4\gamma^2\hbar^2\omega^2}\right], \tag{14a}$$

$$\mathrm{Im}\chi_{nn'}(\omega)=\frac{1}{4\pi b}\begin{cases}\arctan[2\gamma\hbar\omega/\hbar^2(\omega^2-\omega_1^2)]-\arctan[2\gamma\hbar\omega/\hbar^2(\omega^2-\omega_2^2)], & \hbar\omega\leqslant\hbar\omega_1\\ \arctan[2\gamma\hbar\omega/\hbar^2(\omega^2-\omega_1^2)]-\arctan[2\gamma\hbar\omega/\hbar^2(\omega^2-\omega_2^2)]-\pi, & \hbar\omega_1<\hbar\omega<\hbar\omega_2\\ \arctan[2\gamma\hbar\omega/\hbar^2(\omega^2-\omega_1^2)]-\arctan[2\gamma\hbar\omega/\hbar^2(\omega^2-\omega_2^2)], & \hbar\omega\geqslant\hbar\omega_2,\end{cases} \tag{14b}$$

where

$$b=(\hbar^2/2)[1/m_n^*-1/m_{n'}^*], \tag{15a}$$

$$\hbar^2\omega_1^2=(\hbar^2/2m_{n'}^*)^2(k_{nF}^2-k_{n'F}^2)^2+\gamma^2, \tag{15b}$$

$$\hbar^2\omega_2^2=(\hbar^2/2m_n^*)^2(k_{nF}^2-k_{n'F}^2)^2+\gamma^2. \tag{15c}$$

Here, k_{nF} and $k_{n'F}$ are the Fermi wave numbers for subband n and subband n', respectively. The imaginary part in Eq. (14b) will contribute directly to the absorption. The transition in Eq. (15b) is from the Fermi edge of subband n, while the transition in Eq. (15c) is to the Fermi edge of subband n'. When only the two lowest subbands are occupied, the low-energy single-particle excitations clearly correspond to the transition from the Fermi edge of subband 1 to the second subband, and the transition to the Fermi edge of subband 2 from the first subband. These excitations are shown schematically in Fig. 1. There is a doublet structure at $T=0$ K

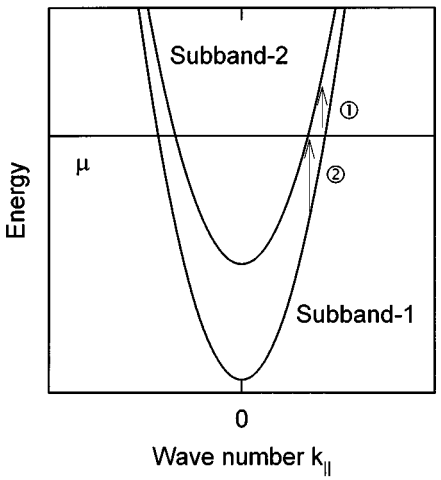

FIG. 1. Schematic of the single-particle transitions when only the two lowest tunneling-split subbands are occupied. These correspond to the transition from the Fermi edge of subband 1 to the second subband, denoted as 1, and the transition to the Fermi edge of subband 2 from the first subband, denoted as 2. The subband energies are $E_{n,k_{\|}}=E_n+\hbar^2k_{\|}^2/2m_n^*$ $(n=1,2)$ with $m_2^*>m_1^*$.

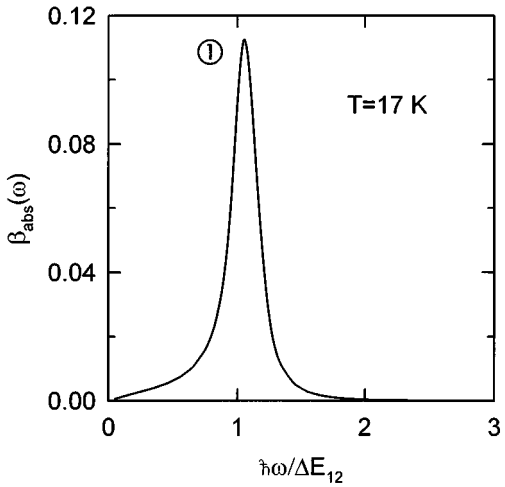

FIG. 2. The absorption coefficient (in units of 10^3 cm^{-1}) for a double-quantum-well structure at $T=17$ K as a function of the incident photon energy expressed in terms of the ground-state tunneling-splitting $\Delta E_{12}=2.74$ meV. The middle barrier has width 40 Å and each quantum well is 75 Å wide. The barriers are uniformly doped and have a volume dopant density of 10.0×10^{17} cm^{-3}. Here, 1 denotes the peak containing the two unresolved peaks for the transition from the Fermi edge of subband 1 and the transition to the Fermi edge of subband 2.

peaked at $\hbar\omega=\hbar\omega_1$ and $\hbar\omega_2$, respectively. There is no singularity in the imaginary part in Eq. (14b) even when the broadening goes to zero. However, when the condition

$$\gamma=\frac{\pi\hbar}{16}\left[\frac{(\omega_2-\omega_1)(\omega_2+3\omega_1)(3\omega_2+\omega_1)}{(\omega_2+\omega_1)^2}\right] \tag{16}$$

is met, the doublet structure should be best resolved. The logarithmic singularities in Eq. (14a) will change the screening significantly and occur as two plasmon excitation modes. When $T=0$ K, we found that the peak strength at $\hbar\omega=\hbar\omega_1$ is larger than that at $\hbar\omega=\hbar\omega_2$.

The appearance of a doublet structure at high temperature is understood as follows. At high temperatures, there are two additional contributions to the optical absorption coefficient that make the appearance of a doublet structure easily observed. As a result of thermal depopulation at finite temperatures, there will be additional unoccupied states in subband 2 and occupied states in subband 1 both below and above the Fermi level at $T=0K$. Since $m_2^*>m_1^*$, this causes a downward shift of the transition peak 1 and, at the same time, an upward shift of the transition peak 2. Consequently, the peak separation increases with the temperature, which is the major reason for the observation of a doublet structure in the absorption coefficient at high temperatures. Since the transition between large-k states has larger oscillator strength, we can easily understand that an imbalance will be introduced by the finite temperature between the strength of peak 1 and peak 2. Therefore, the transition peak 2 only occurs as a shoulder on the high-energy side of the peak 1.

The bare confining potential $V_b(z)$ is zero inside the well and 0.26 eV outside. The background dielectric constant and the electron effective mass for the bulk material making up the barrier region is taken as 12.0 and $m_B=0.08m_e$, respectively, where m_e is the free-electron mass. The corresponding parameters for the well region were taken as 13.0 and $m_W=0.67m_e$. We chose the parameter representing the effect due to scattering in the polarization function as $\gamma=0.1\Delta E_{12}=0.275$ meV, where ΔE_{12} is the separation between the two lowest subband edges. From the self-consistent Hartree calculation, we find that only the two lowest tunneling-split subband edges lie below the chemical potential at all temperatures from 0 to 300 K for a dopant concentration 2.4×10^{12} cm^{-2}. However, when the dopant concentration increases to 6.0×10^{12} cm^{-2}, all four tunneling-split subband edges are below the chemical potential in the same temperature range. If we are only concerned with the low-energy excitations in DQW's, we find that the only two possible tunneling-split intersubband transitions are $1\rightarrow2$ (denoted as peak-1) and $1'\rightarrow2'$ (denoted as peak $-1'$).

In Fig. 2, we show plots of the absorption coefficient $\beta_{\rm abs}(\omega)$ and its frequency derivative as a function of the photon energy $\hbar\omega$ at $T=17$ K. From it, we see only one high-energy peak 1 for the energy range shown here because only the subband 1 and 2 are populated. Peak 1 actually contains two unresolved peaks due to their small separation and relatively large broadening. When the relaxation time increases, the condition in Eq. (16) will be met. Therefore, the splitting of these two peaks can be accomplished. The lower one corresponds to the transition from the Fermi edge of subband 1, and the upper one is for the transition to the Fermi edge of subband 2. The left-side edge of peak 1 is determined by the number of thermally excited electrons above the Fermi edge of subband 1, while the right-side edge is decided by the number of ''hole'' states created below the Fermi edge of subband 2. The slight asymmetry in the line shape is due to the large-k states of thermally excited electrons above the Fermi edge of subband 1, which gives larger oscillator strength as $m_2^*>m_1^*$. The peak broadening and many-body depolarization effect slightly shift peak 1 above the separation ΔE_{12} between the two lowest subband edges.

In Fig. 3, we show plots of the absorption coefficient

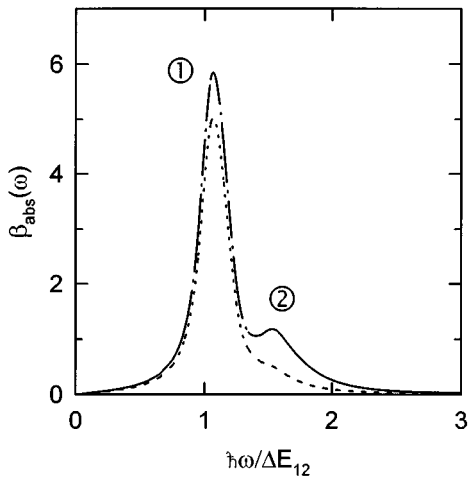

FIG. 3. The same as Fig. 2 except that $T=300$ K (dashed line) and $T=400$ K (dashed-dotted line). The same energy scale $\Delta E_{12}=2.74$ meV as in Fig. 2 is used. Here, 1 and 2 denote the resolved low and high peaks split from the previous unresolved peak 1 of Fig. 2, respectively.

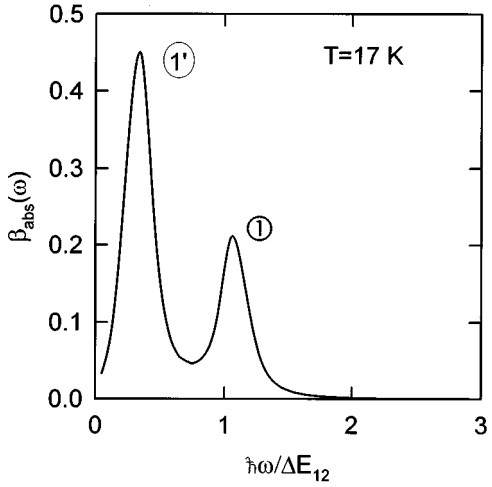

FIG. 4. The absorption coefficient (in units of 10^3 cm^{-1}) at $T=17$ K as a function of the incident photon energy expressed in terms of the energy scale $\Delta E_{12}=2.74$ meV. The middle barrier is 40 Å wide and each quantum well has width 75 Å. The barriers are uniformly doped and have a volume dopant density of 25.0×10^{17} cm^{-3}. Here, $1'$ denotes the peak containing the two unresolved peaks for the transition from the Fermi edge of subband $1'$ and the transition to the Fermi edge of subband $2'$, which are the tunneling-split originally degenerate first excited state in the isolated quantum wells.

$\beta_{abs}(\omega)$ at $T=300$ K and at $T=400$ K as a function of the photon energy $\hbar\omega$. In this case, we find for the energy range shown here that peak 1 is resolved into a doublet. At $T=300$ K, a high-energy shoulder ''2'' occurs in the spectrum. With the increase of temperature, the peak strength of this shoulder ''2'' increases and a pair of split peaks becomes clear. At the same time, the separation between the split peaks increases due to more ''hole'' states being created around the Fermi edge of subband 2 at high temperatures compared with those around the Fermi edge of subband 1 as $m_2^*>m_1^*$. The difference between ω_1 and ω_2 increases. Consequently, the condition in Eq. (16) becomes more easily satisfied. Both the transfer of the peak strength from ''1'' to ''2'' and the increased peak separation make it possible for us to observe the doublet structure in Fig. 3. Although the peak position becomes insensitive at high temperatures, the peak strength still increases with the temperature as explained above.

Figure 4 shows a plot of $\beta_{abs}(\omega)$ as a function of the incident photon energy $\hbar\omega$ at $T=17$ K for high dopant charge density 6.0×10^{12} cm^{-2}. The energies of the four lowest energy levels at this increased density below the chemical potential are $E_1=0.2861$ eV, $E_2=0.2881$ eV, $E_{1'}=0.3453$ eV, and $E_{2'}=0.3460$ eV. The tunneling splitting in the excited states $1'$ and $2'$ is suppressed by the Hartree interaction. This will shift down the peak positions at $\omega=\omega_1$ and ω_2. Compared with Fig. 2, the high dopant density allows electrons to populate subbands $1'$ and $2'$. As a result, another new unresolved peak $1'$ becomes visible on the low-energy side besides the previous unresolved peak 1 in the spectrum. The peak strength of peak 1 increases slightly with the dopant density. The broadening of peak 1 is reduced compared with Fig. 2 because the difference of Fermi wave vectors for subbands 1 and 2 decreases with the total electron density when $m_2^*>m_1^*$. Moreover, we find the broadening of peak $1'$ is smaller than that of peak 1. This is because the effective mass of the electrons in the excited state $1'$ and $2'$ is larger than in the tunneling split ground state 1 and 2. It is also due to the small tunneling splitting between the excited state $1'$ and $2'$. The peak strength of peak $1'$ is larger compared to that of peak 1. This also results from the small split peak separation inside the unresolved peak $1'$ which increases the overlap of the two unresolved peaks inside peak $1'$.

The authors acknowledge the support in part from the City University of New York PSC-CUNY Grant No. 664279. The work of D.N.T. was supported in part by the National Research Council Associateship Program, National Science Foundation Grant No. ECS-9521659, Research Corporation, and by the American Chemical Society (Petroleum Research).

*Also at The Graduate School and University Center of the City University of New York, New York, NY 10036.

[1] M. Załużny, Solid State Commun. **82**, 565 (1992).
[2] M. Załużny, Phys. Rev. B **43**, 4511 (1991).
[3] G. Gumbs, D. Huang, and J. P. Loehr, Phys. Rev. B **51**, 4321 (1995).
[4] G. Gumbs and G. Ăizin, Phys. Rev. B **51**, 7074 (1995).
[5] G. Ăizin and G. Gumbs, Phys. Rev. B **52**, 1890 (1995).
[6] M. O. Manasreh and J. P. Loehr, in *Semiconductor Quantum Wells and Superlattices for Long Wavelength Infrared Detection*, edited by M. O. Manasreh (Artech, MA, 1993), Chap. 2.
[7] P. von Allmen, M. Berz, F. K. Reinhart, and G. Harbeke, Superlattices Microstruct. **5**, 259 (1989).
[8] P. von Allmen, M. Berz, G. Petrocelli, F. K. Reinhart, and G. Harbeke, Semicond. Sci. Technol. **3**, 1211 (1988).
[9] U. Ekenberg, Phys. Rev. B **36**, 6152 (1987).